

CHAPTER IV RESULTS AND DISCUSSION

4.1 Carbon-Nitric Oxide Reaction

4.1.1 Determination of TOF

From the thermogravimetric analyzer (TGA) results as shown in Figure 4.1, the rates of weight change in graphite during NO gasification reaction were measured with time.

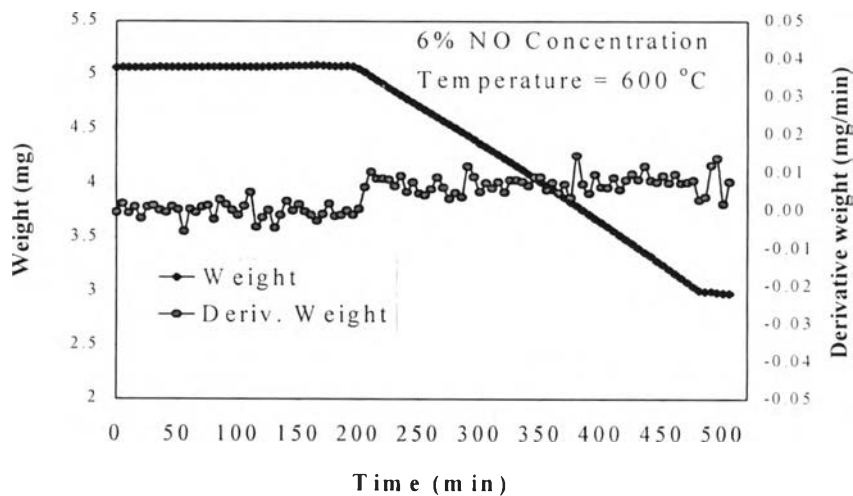


Figure 4.1 Typical TGA result of NO reduction on Micro 850 graphite.

Figure 4.1 shows the mass reduction data obtained from TGA experiment. The result indicates that the reaction rate changes at low burn-off levels and then becomes constant in the range from 10% to 20% burn-off levels. However, the reaction rate changes again at high burn-off levels. The reaction rates between 10% to 20% burn-off were used in this work. In fact the reaction rates were determined based on a basis of mass or surface area unit. However, it was indicated that edge atoms on carbon

surfaces are active sites for gasification (Chen and Yang, 1993). Thus, the reactivity should be considered based upon the actual active surface area rather than the total surface area. In this study, The reactivities of graphite were determined in terms of turnover frequency (TOF), that is, the reaction rate based on per active sites. Turnover frequency (TOF) was determined by using the rates of carbon atoms gasified and the number of active sites. Due to the fact that a sample used in this study was graphite with well-defined structure and that the edge atoms on the edge plane surface areas are the active sites of the NO-carbon reaction. Therefore, the determination of edge plane surface areas and the number of edge atoms that can be calculated from the geometry of the graphite flakes is described in Appendix A.

4.1.2 Effect of Temperature and NO Concentration on TOF

The effects of temperature and NO concentration on TOF are shown in Figure 4.2.

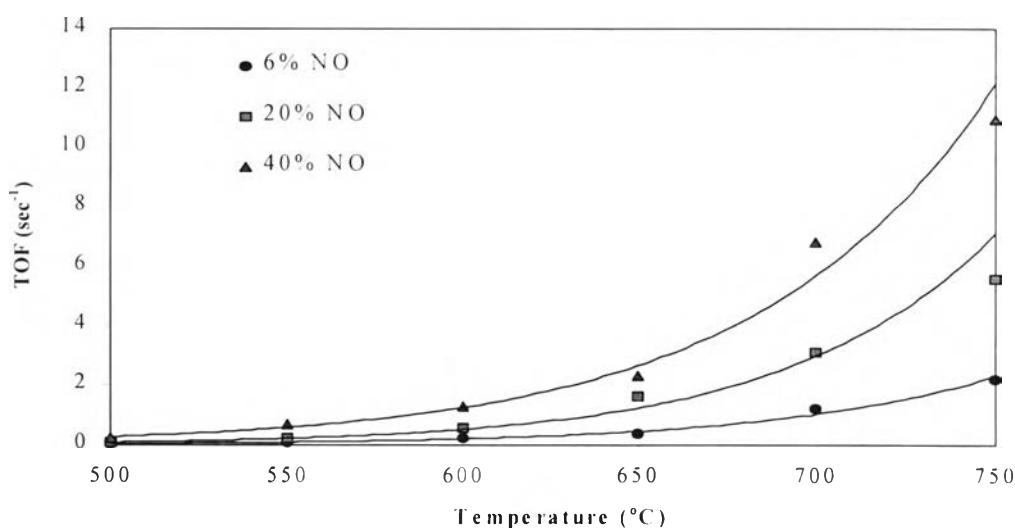


Figure 4.2 Effects of gasification temperature and NO concentration on TOF for Micro 850 graphite.

The results show that at constant NO concentration, TOF is increased when either gasification temperature or NO concentration increases. These

results indicate that both the reaction temperature and the NO concentration have affected on the TOF. The reaction temperature and initial NO concentration dependence of TOF can be expressed by the following equation:

$$\text{TOF} = A_0 P_{\text{NO}}^n e^{-E_a/RT} \quad (4.1)$$

where A_0 is the pre-exponential factor, n is the reaction order with respect to NO partial pressure, P_{NO} is the NO partial pressure, E_a is the activation energy, R is the universal gas constant, T is the reaction temperature.

4.1.3 Kinetic Studies

4.1.3.1 Activation Energy

The typical power rate law for the NO gasification rate equation can be expressed as follows:

$$\text{TOF} = k P_{\text{NO}}^n \quad (4.2)$$

where TOF is the turnover frequency or rate per active site, k is the reaction rate constant, P_{NO} is the NO partial pressure, n is the reaction order with respect to NO partial pressure.

The Arrhenius equation can be shown as follows:

$$k = A_0 e^{-E_a/RT} \quad (4.3)$$

where k is the reaction rate constant, A_0 is the pre-exponential factor. E_a is the activation energy (kJ/mol), R is the gas constant of 8.314 J/mol K. T is the absolute temperature (K). By substituting Eq.(4.3) into Eq.(4.2) gives Eq.(4.1) and then by taking the natural logarithm on both sides of Eq.(4.1) yields

$$\ln \text{TOF} = \ln(A_0 P_{\text{NO}}^n) - \frac{E_a}{R} \left(\frac{1}{T} \right) \quad (4.4)$$

The activation energy can be determined from Eq.(4.4) by plotting $\ln \text{TOF}$ versus $1/T$. A slope of straight line is proportional to the activation energy. The Arrhenius plots of Micro 850 graphite are shown in Figures 4.3-4.5.

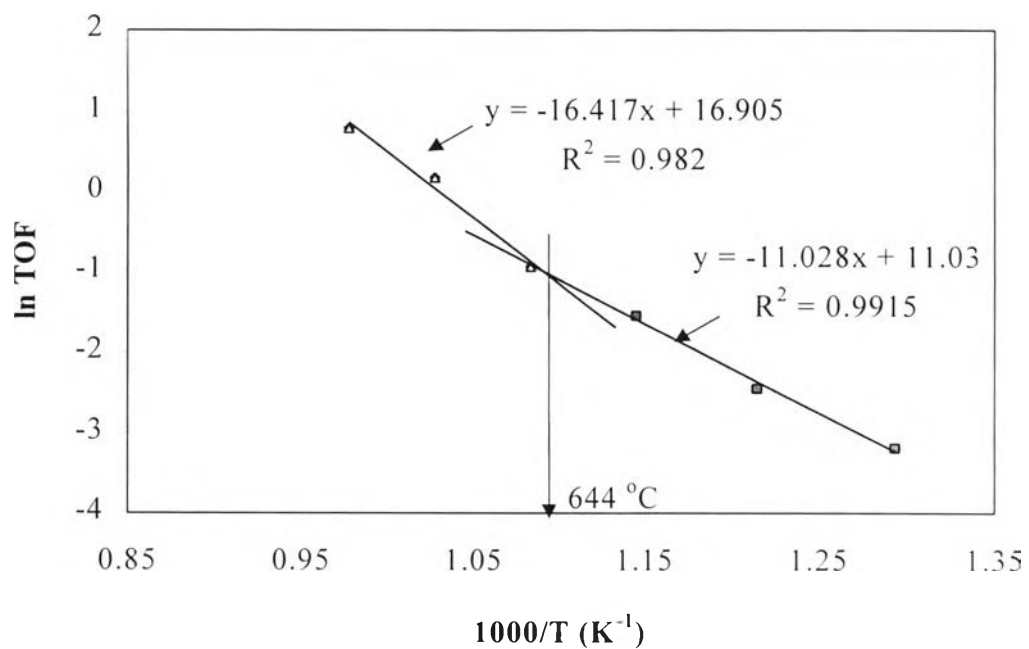


Figure 4.3 Arrhenius plot of Micro 850 graphite at 6 % NO concentration.

Figure 4.3 shows the Arrhenius plots of Micro 850 graphite at 6 % NO concentration. It is interesting to note that there is a distinctive change in the slopes of Arrhenius plots. The temperature at which there is a distinctive change in the slopes of Arrhenius plots at is called the temperature break. It has been found to occur at about 644 °C. The observation of a break point in the Arrhenius plot has reported by Li *et al.* (1998). They concluded that the transition temperature was noticed to occur in the temperature range of

600-680 °C. At temperatures lower than the temperature break (the low temperature regime (<644 °C)), the activation energy of the reaction which increases with an increase in the reaction temperature shows the activation energy of 92 kJ/mol. While above the temperature break (the high temperature regime >623 °C), the activation energy which also increases with increasing the reaction temperature inhibits the activation energy of 136 kJ/mol. Generally speaking, it can be obviously described that at higher temperatures the activation energy is found to have higher value than that in lower temperature regime.

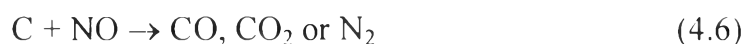
The reason for the change in the activation energy and this temperature break in the Arrhenius plot is not well understood. But it is believed that the increase in the activation energy might be attributed to a change in the reaction mechanism (Furusawa *et al.*, 1980). Chen *et al.*, (1998) explained the NO-reaction in two temperature regimes can be controlled or dominated by different elementary processes with different activation energies. They suggested that when the basal plane of graphite sample is exposed to reactant gas, a single vacancy on the basal plane, which is surrounded by three edge atoms, can be expanded to form an etch pit, and this pit is one atomic large deep, that is 3.35 \AA . The graphite gasification reactions take place through this type of edge recession process. Besides the monolayer etch pit formation, there are other processes that also take place during carbon gasification reactions. Therefore, the reaction rate for this process is the intrinsic rate for edge site etch process. The C-attack, or basal plane atom abstraction, causes the formation of nascent pits with smaller diameters. For the C-NO reaction, formation of nascent pits becomes significant at temperatures higher than 750 °C. The contribution by the nascent pit formation to the overall gasification rate increases with temperature. In addition, multilayer pits are sometimes observed and are usually caused by the screw dislocation in the graphite crystal where cooperative effects (among adjacent

layers) can be involved. The multilayer pits are observed only at high temperature. Screw dislocations are actually a combination of many vacancies on different layers, and they are much more reactive than a single vacancy under the whole temperature range. The formation of nascent and deep pits with higher activation energies (than that for monolayer etching) contributed to the higher apparent activation energy in the high temperature range.

The temperature break indicates a change in the reaction mechanism (Teng *et al.*, 1992). They described that the gasification of carbon by NO involves two parallel process: The low-temperature regime (arbitrarily < 650 °C or 923 K) is exhibited by a non-constant activation energy in the range of 63-88 kJ/mol. This regime involves somewhat slow desorption of relatively stable surface complexes as follows:



The NO-carbon reaction in the high-temperature regime (again, arbitrarily > 923K) has a constant activation energy of 180 kJ/mol. The process is also believed to involve NO attack on active unoccupied sites and then, a prompt product release step, following the rate-controlling formation of surface complexes formed by reaction with NO. This process is in an apparently single-step process:



These two different mechanism has the different activation energy. Therefore the activation energy increased when reaction took place above approximately 644 °C as a result of different mechanism.

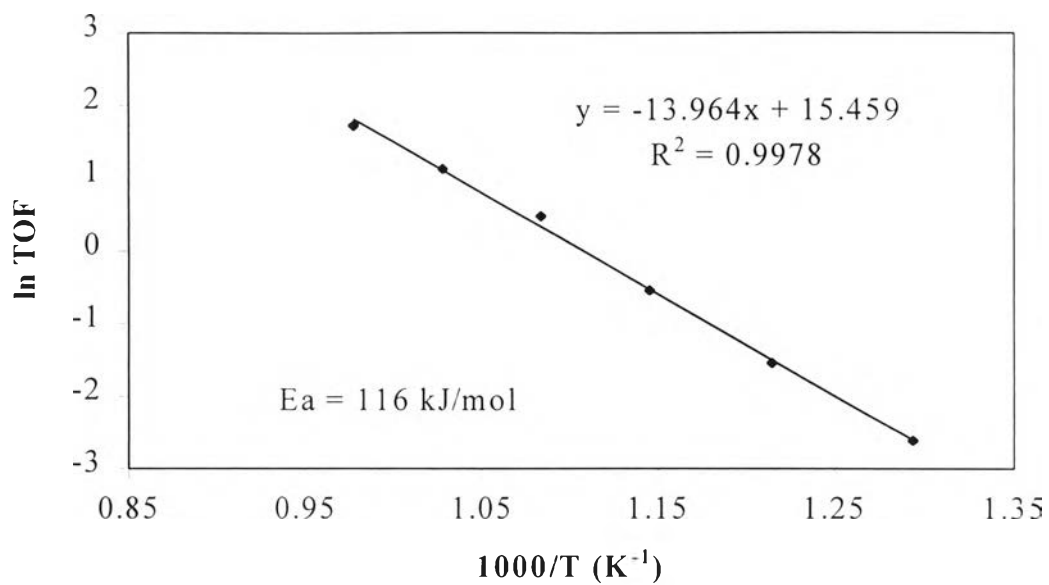


Figure 4.4 Arrhenius plot of Micro 850 graphite at 20% NO concentration.

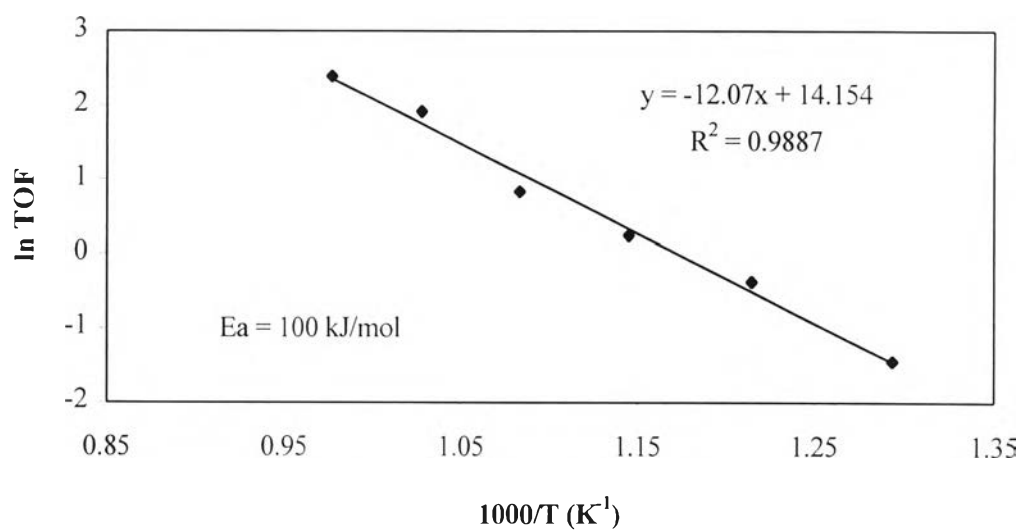


Figure 4.5 Arrhenius plot of Micro 850 graphite at 40% NO concentration.

Figures 4.4 and 4.5 show the Arrhenius plot of the NO reduction in the temperature range of 500-750 °C at 20% and 40% NO concentration, respectively. It is interesting to notice that neither 20% nor 40% NO concentration had appeared a temperature break in each Arrhenius plots. The activation energies were 116 and 100 kJ/mol for 20% and 40% NO concentration, respectively.

The reason for the absence of a temperature break in the Arrhenius plot at NO concentrations greater than 6% may be due to an increase in the number of NO molecules to attack on occupied sites. At high concentration of NO, NO molecules can easily attack on active sites. Thus, the process at high concentration may be the process involved NO attack on active sites followed by a fast release of products. This process controls the overall gasification rate in the range of temperature considered resulting in the absence of break on the Arrhenius plot. The activation energies investigated in this work are presented in Table 4.1.

Table 4.1 The activation energy for the carbon-NO reaction in the temperature range of 500-750 °C by using Micro 850 graphite.

% NO concentration	E _a (kJ/mol)	
	Low temp.	High temp.
6	92	136
20	-	116
40	-	100

Table 4.1 shows the activation energies in the range of 500-750 °C for 6%, 20%, and 40% NO concentration. The results indicate that the activation energy obtained from this sample is in the range of 100-136 kJ/mol. Moreover, the results show that the activation energy for 40% NO

concentration is lower than that for 20%. Therefore, the carbon-NO reaction is more favorable at higher NO concentrations. As described previously, at high concentration of NO molecules of NO have more chances to attack on active sites so that the reaction readily occurs. This is a reason why the activation energy for higher NO concentration is lower than that for lower concentration.

4.1.3.2 Reaction Order

The characterized power rate law for the carbon gasification in NO could be followed by Eq.(4.2). By taking the natural logarithm on Eq. (4.2) gives

$$\ln \text{TOF} = \ln k + n \ln P_{\text{NO}} \quad (4.7)$$

Thus, the reaction order can be investigated from the slope of a plot between $\ln \text{TOF}$ and $\ln P_{\text{NO}}$. Relationships between NO partial pressure and TOF for NO reduction on Micro 850 graphite are shown in Figure 4.6.

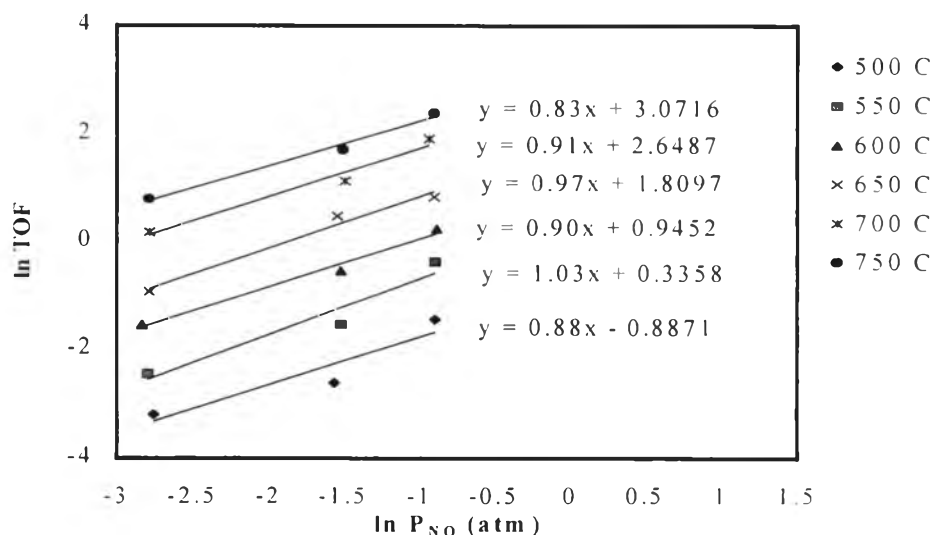


Figure 4.6 Correlations between NO partial pressure and TOF for NO reduction on Micro 850 graphite in the temperature range of 500-750 °C.

Figure 4.6 depicts the kinetic order of NO reduction by Micro 850 graphite with respect to NO concentration. It can be obviously delineated that straight lines are acquired for this sample. Also, it can be noticed that the slopes of the plots are close to unity. This means the reaction is very nearly first-order with respect to NO at temperature below 644 °C (low temperature regime). Conversely, the slopes between 0.7 and 0.9 have been observed at temperature above 644 °C (high temperature regime). This is believed to the fact that the influence of CO has on the reaction rate (Aarna and Suuberg 1997; Furusawa *et al.*, 1980, 1985). CO was in fact observed as a dominant product at higher temperatures. Unfortunately, this CO appearing as a product can subsequently react by the possibility of surface catalyzed reaction. Accordingly, CO can behave as both product and reactant gases simultaneously. Aarna and Suuberg (1997) found that even low levels of CO can significantly affect the observed reaction order. Therefore, the reaction order with respect to NO was decreased due to the presence of CO in the high temperature regime.

The kinetic parameters for carbon-nitric oxide reaction by using various carbons were collected in Table 4.2. It is interesting to observe that the reactions between NO reactant and graphite give higher in the activation energies than in other materials. This implies that a graphite as carbon material has low activity and also imply that the activation energy depends significantly on a material used for the study. It is also seen that the kinetic parameters determined in this study are in good agreement with those in other studies (Aarna and Suuberg, 1997). The temperature break is another one to observe in this study. The break points for SP-1, Micro 850 and Micro 450 graphite are shown in Figure 4.7.

Table 4.2 Comparison of kinetic parameters of the carbon-NO reaction using Micro 850 graphite with other studies (Aarna and Suuberg, 1997).

Carbon type	Reactor	Temperature range (K)	P _{NO} (kPa)	E _a (kJ/mol)		Reaction order	Surface area (m ² /g)
				Low temp	High temp		
Graphite	Fixed bed	873-1173	0.04-0.90	-	239	1	3.7
Graphite	Fixed bed	973-1223	0.05-0.15	-	162.7	-	13
Graphite	TGA	873-1223	1.0-8.1	65	200	1	17-100
Graphon	Fixed bed	1027-1233	0.27-0.75	-	86.6	1	87
Graphite	Fixed bed	950-1250	0.1-0.15	-	240	-	2
PF-char	TGA	723-1173	1.0-8.1	35	140	-	525-878
PF-char	TGA	773-1073	1.0-10.1	63-88	180	1	2-400
Micro 450	TGA	773-1073	6.0	63.8	109.2	1	0.89
Micro 450	TGA	773-1073	20.0	-	87.8	1	0.89
Micro 450	TGA	773-1073	40.0	-	79.9	1	0.89
SP-1	TGA	773-1073	6.0	83.6	122.4	1	0.054
SP-1	TGA	773-1073	20.0	-	93.4	1	0.054
SP-1	TGA	773-1073	40.0	-	83.2	1	0.054
Micro 850	TGA	773-1073	6.0	92	136	1	0.45
Micro 850	TGA	773-1073	20.0	-	116	1	0.45
Micro 850	TGA	773-1073	40.0	-	100	1	0.45
Activated carbon	Fixed bed	773-1118	0.03-0.20	63.5	181	1	800-1200
Cellulose char	TGA	773-923	10.1	-	64	-	-
Coconut char	TGA	673-1173	1.0-8.1	42	120	-	2682

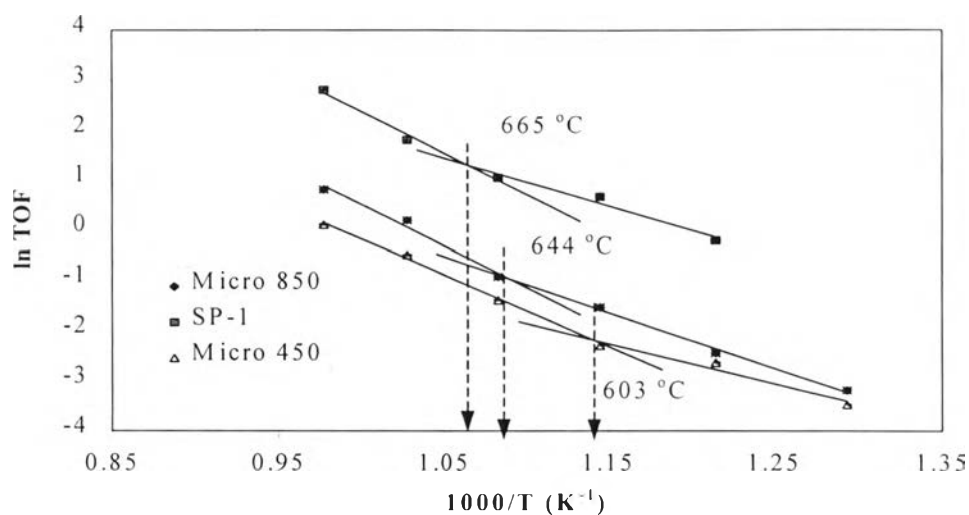


Figure 4.7 Comparison of break temperatures in SP-1, Micro 450, and Micro 850 graphites at 6% NO concentration.

Figure 4.7 shows the Arrhenius plots of SP-1, Micro 450 and Micro 850 graphite sample at 6% NO concentration. TOF data for the SP-1 and Micro 450 graphite samples were obtained from the previous work (Tatiyakiatisakun, 1998). As can be seen there is a distinctive change in slope of Arrhenius plots. The break temperatures can be observed at 665, 644, and 603 °C for SP-1, Micro 850 and Micro 450, respectively.

4.2 Carbon-Nitrous Oxide Reaction

4.2.1 Determination of TOF

Like the carbon-N₂O reaction, the rates of weight change in graphite during N₂O gasification reaction, as shown in Figure 4.8, are measured with time. Turnover frequency was determined by using the rates of carbon atoms gasified and the number of active sites. The determination of the number of active sites, that is, that of the number of edge atoms as active sites can be explained in Appendix A.

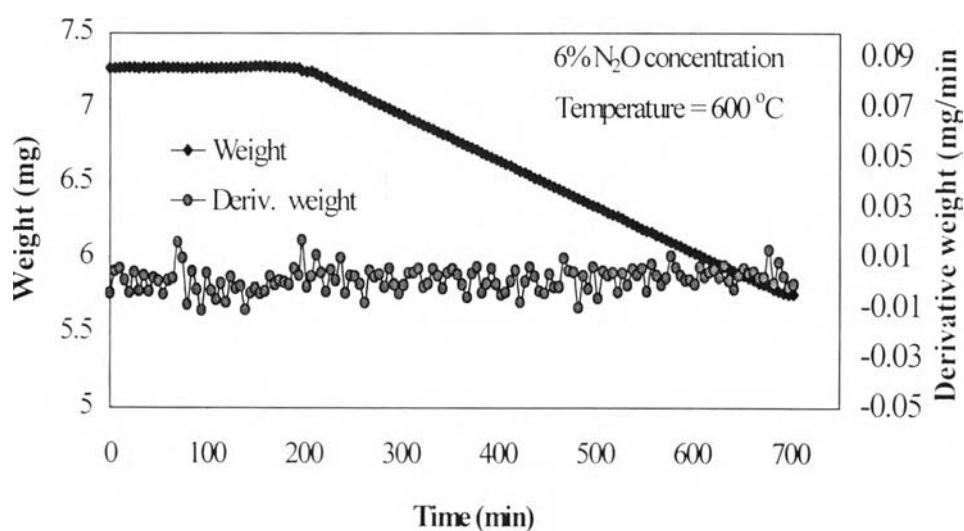


Figure 4.8 Typical TGA result of N₂O reduction on Micro 850 graphite.

Figure 4.8 illustrates the mass reduction data obtained from TGA experiments. The results show that the reaction rate changes at very low burn-off levels and then runs constant in the range from 10% to 20% burn-off levels. However, the reaction rate changes again at very high burn-off levels. Thus, only reaction rates between 10% and 20% burn-off were employed in this study.

4.2.2 Effect of Temperature and N₂O Concentration on TOF

The effects of reaction temperature and N₂O concentration at 6%, 12%, and 20% N₂O concentration are shown in Figure 4.9.

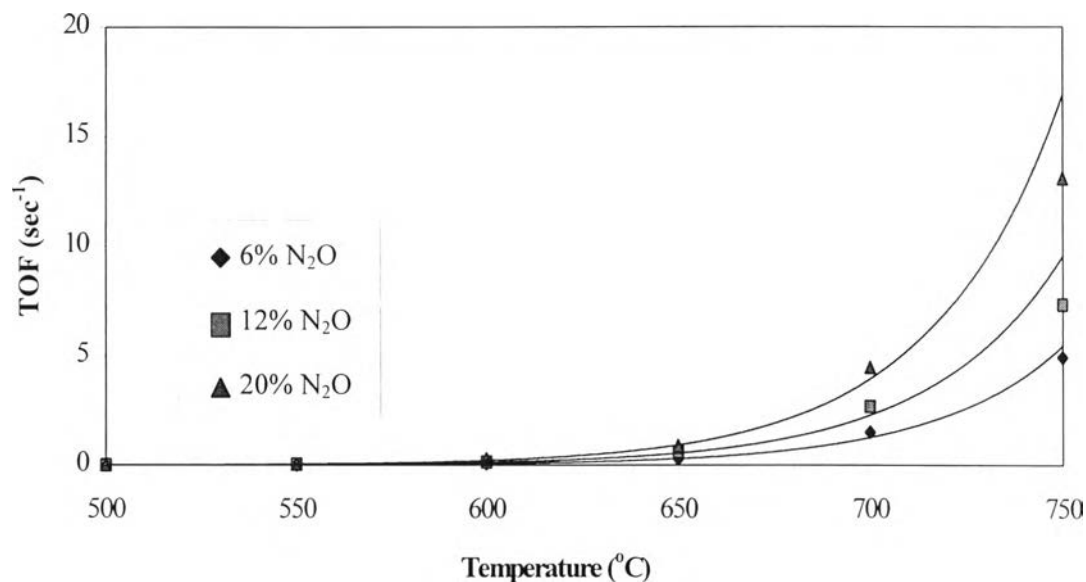


Figure 4.9 Effect of reaction temperature and N₂O concentration on TOF for N₂O reduction on Micro 850 graphite.

Figure 4.9 shows the effects of reaction temperature and N₂O concentration on TOF for N₂O reduction by Micro 850 graphite. It is depicted that at constant N₂O concentration TOF is increased when either reaction temperature or N₂O concentration increases. These results imply that both the gasification temperature and N₂O concentration have influenced on TOF.

4.2.3 Kinetic Studies

4.2.3.1 Activation Energy

The activation energy can be determined from Eq.(4.4) by plotting \ln TOF versus $1/T$ or Arrhenius plot. A slope straight line is proportional to the activation energy. The Arrhenius plot of Micro 850 graphite at 6%, 12%, and 20% N₂O concentration is shown in Figure 4.10.

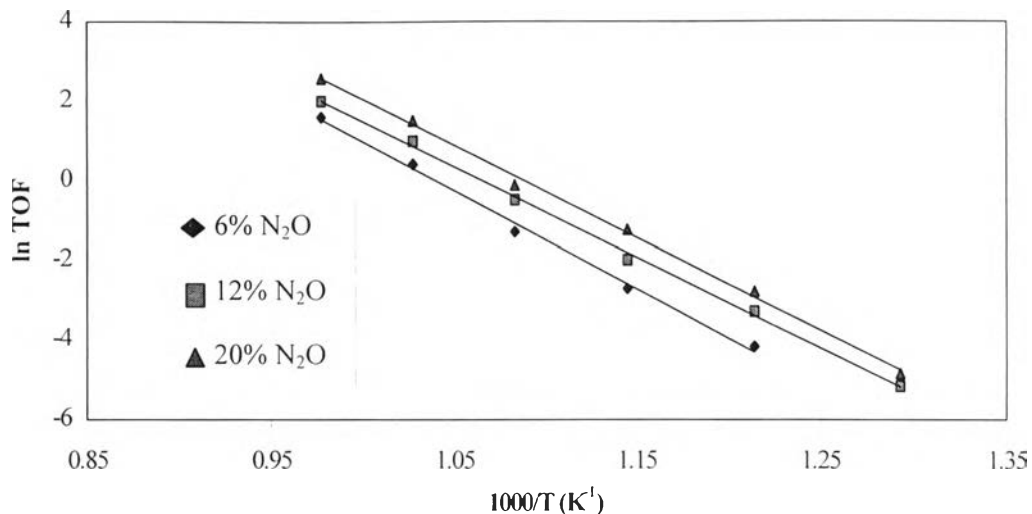


Figure 4.10 Arrhenius plot of Micro 850 graphite at 6%, 12%, and 20% N₂O concentration.

It is interesting to observe from Figure 4.10 that at 6%, 12%, and 20% N₂O concentrations there is no change in the activation energy for the entire range of temperatures employed for this study. This implies that a change in the reaction mechanism is not appeared. Teng *et al.* (1997) studied the global kinetics of the carbon gasification in N₂O by a thermogravimetric system. They found that the temperature break had observed to appear about 748 K. In this study, the transition temperature had not be found owing to the fact that the temperature range of 773-1073 K used in this work is out of the break point noticed in the work of Teng *et al.* (1997). The activation energies determined in this study could be collected in Table 4.3.

Table 4.3 The activation energy for carbon-N₂O reaction in the temperature range of 500-750 °C by using Micro 850 graphite.

% N ₂ O concentration	E _a (kJ/mol)	
	Low temp	High temp
6	-	204
12	-	196
20	-	192

Table 4.3 shows the activation energy for carbon- N₂O reaction in the temperature range of 500-750 °C by using Micro 850 graphite. It is depicted that the activation energies obtained from this study are in the range of 192-204 kJ/mol. In addition, the results show that the activation energy for 20% N₂O concentration is lower than that for 12% N₂O concentration. This indicates that the carbon gasification in N₂O is more favorable at higher N₂O concentrations. This may be due to the fact that more molecules of N₂O at higher concentrations are potentially able to attack active sites when compared to those at lower N₂O concentrations.

4.2.3.2 Reaction Order

The reaction order of carbon- N₂O reaction can be investigated from Eq.(4.7) by plotting ln TOF versus ln P_{N₂O}. The slope of straight line in relationship between ln TOF versus ln P_{N₂O} is proportional to the reaction order. The correlations between the N₂O partial pressure and TOF for N₂O reduction on Micro 850 graphite are shown in Figure 4.11.

Figure 4.11 shows the relationships between N₂O partial pressure and TOF for N₂O reduction on Micro 850 graphite. The slope of each line presented the reaction order with respect to N₂O partial pressure is close to unity. This implies that the N₂O reduction by Micro 850 graphite is a first

order reaction with respect to N_2O pressure. The kinetic parameters brought to compare with those of other work are summarized in Table 4.4.

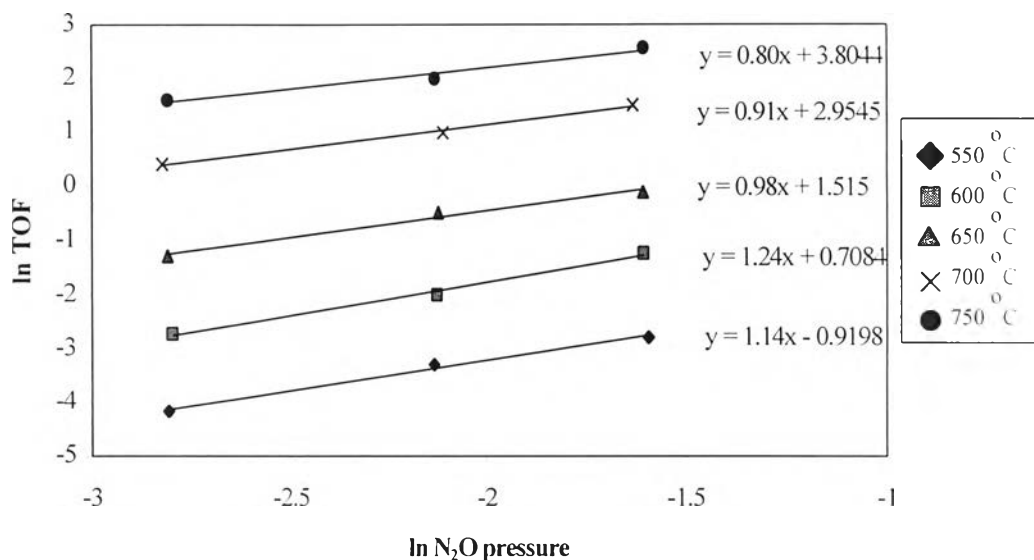


Figure 4.11 Correlations between N_2O partial pressure and TOF for N_2O reduction on Micro 850 graphite in the range temperature of 500-750 °C.

Table 4.4 shows the kinetic parameters for carbon- N_2O reaction by using various types of carbon. As seen in Table 4.4, a variation of the activation energies with temperature is not found in any work. One of the reasons can be attributed to the different techniques employed in determining the reaction rate. The other workers determined the reaction rate based on the disappearance of N_2O in the reaction streams, whereas the reaction rate was determined according to the carbon consumption in the present study. It is possible that N_2O decomposition can be catalyzed on the carbon surface and proceeds without carbon consumption (Wójtowicz *et al.*, 1993). Notice that the activation energies for graphite are higher than those for other carbon materials. This implies that graphite has the lowest reactivity and the highest activation energy.

Table 4.4 Comparison of kinetic parameters of the N₂O carbon reaction using Micro 850 graphite with other studies (Teng *et al.*, 1997).

Carbon type	Reactor	Temperature range (K)	N ₂ O pressure (kPa)	E _a (kJ/mol)	Reaction order
Charcoal	Static reaction bulb	551-653	1-52	134	1
Charcoal	Circulated batch	673-873	0.26-46	176	1
Graphon	Circulated batch	673-923	0.17-50	284	1
Cedar Grove bit. Char	Fixed bed	700-1250	0.008	116	-
Prosper bit. Char	Fixed bed	700-1250	0.008	101	-
Eschweiler bit. Char	Fixed bed	700-1250	0.008	83.1	-
Norit RX act. Carbon	Packed bed	640-720	0.0035-0.0045	96 ₊₁₃	-
DE53 lignite char	Fixed bed	673-1223	0.019-0.19	77 ₊₂₃	0.59 _{+0.43}
Gardanne subbit. Char	Fixed bed	673-1223	0.019-0.19	68 ₊₂₇	0.58 _{+0.59}
Daw-Mill bit. Char	Fixed bed	673-1223	0.019-0.19	77 ₊₁₇	0.59 _{+0.34}
Blanzky anthr. Char	Fixed bed	673-1223	0.019-0.19	66 ₊₉	0.61 _{+0.27}
Norit RX act. Carbon	Fixed bed	673-1223	0.019-0.19	77 ₊₂₃	0.59 _{+0.43}
Micro850	TGA	773-1073	6.0	204	1
Micro 850	TGA	773-1023	12.0	196	1
Micro850	TGA	773-1023	20.0	192	1

4.3 Comparison of Carbon-NO Reaction to Carbon-N₂O Reaction

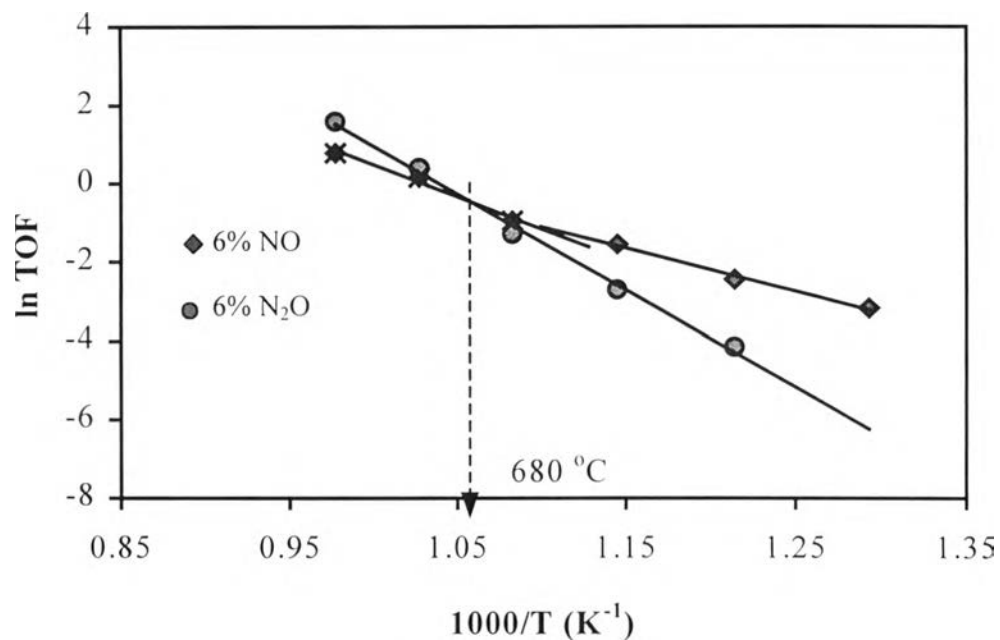


Figure 4.12 Arrhenius plots of Micro 850 graphite for carbon-NO reaction and carbon-N₂O reaction at a reactant concentration of 6%.

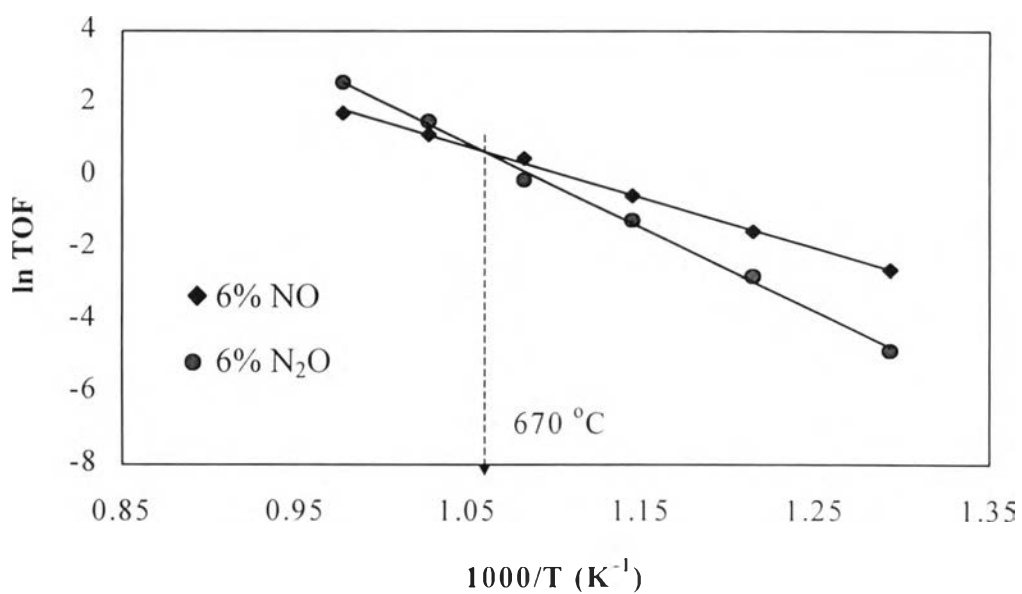


Figure 4.13 Arrhenius plots of Micro 850 graphite for carbon-NO reaction and carbon-N₂O reaction at a reactant concentration of 20%.

Figures 4.12 and 4.13 present the Arrhenius plots for graphite gasification reactions by NO and N₂O in the temperature range of 500-750 °C. These plots indicate that, at above 670 °C, the rates of the carbon gasification in NO are lower than those in N₂O. It is indicated that at this temperature (670 °C), the NO reaction has about the same reaction rate as that of N₂O. Since the N₂O-carbon reaction is considered as an elementary reaction, TOF at this point implies that in the low temperature range, the NO-carbon reaction has the same rate-limiting step as N₂O-carbon does, and it might be the step of desorption of surface complexes (Li *et al.*, 1998). However, in the high temperature range, a significant difference of rate between NO-carbon reaction and N₂O-carbon reaction was found. This indicates that a rate-limiting step is different for the two reactions. Since the same elementary step of N₂O-carbon reaction no longer controls the NO-carbon reaction rate, other factors must be slowing down the NO-carbon reaction rate. There is evidence that the formation of N₂ through NO/N₂O reduction does not involve a surface nitrogen intermediate (Chen *et al.*, 1998). While N₂O can react on the surface to release N₂, the dissociation of NO should involve the coordination between two NO molecules. Therefore, instead of surface desorption, the NO coordination may play a role for the rate-limiting step at high temperatures.